Revisiting the Turbulent Prandtl Number in an Idealized Atmospheric Surface Layer

DAN LI

Program in Atmospheric and Oceanic Sciences, Princeton University, Princeton, New Jersey

GABRIEL G. KATUL

Nicholas School of the Environment, and Department of Civil and Environmental Engineering, Duke University, Durham, North Carolina

SERGEJ S. ZILITINKEVICH

Finnish Meteorological Institute, and Division of Atmospheric Sciences, University of Helsinki, Helsinki, Finland, and Department of Radio Physics, N.I. Lobachevski State University of Nizhniy, Novgorod, and Faculty of Geography, Moscow University, and Institute of Geography, Russian Academy of Sciences, Moscow, Russia, and Nansen Environmental and Remote Sensing Center/Bjerknes Centre for Climate Research, Bergen, Norway

(Manuscript received 10 November 2014, in final form 8 March 2015)

ABSTRACT

Cospectral budgets are used to link the kinetic and potential energy distributions of turbulent eddies, as measured by their spectra, to macroscopic relations between the turbulent Prandtl number (Pr_t) and atmospheric stability measures such as the stability parameter ζ, the gradient Richardson number R_g, or the flux Richardson number R_f in the atmospheric surface layer. The dependence of Pr_t on ζ, R_g, or R_f is shown to be primarily controlled by the ratio of Kolmogorov and Kolmogorov–Obukhov–Corrsin phenomenological constants and a constant associated with isotropization of turbulent flux production that can be independently determined using rapid distortion theory in homogeneous turbulence. Changes in scaling laws of the vertical velocity and air temperature spectra are also shown to affect the Pr_t–ζ (or Pr_t–R_g or Pr_t–R_f) relation. Results suggest that departure of Pr_t from unity under neutral conditions is induced by dissimilarity between momentum and heat in terms of Rotta constants, isotropization constants, and constants in the flux transfer terms. A maximum flux Richardson number R_{fm} predicted from the cospectral budgets method (=0.25) is in good agreement with values in the literature, suggesting that R_{fm} may be tied to the collapse of Kolmogorov spectra instead of laminarization of turbulent flows under stable stratification. The linkages between microscale energy distributions of turbulent eddies and macroscopic relations that are principally determined by dimensional considerations or similarity theories suggest that when these scalewise energy distributions of eddies experience a ''transition'' to other distributions (e.g., when R_f is increased over R_{fm}), dimensional considerations or similarity theories may fail to predict bulk flow properties.

1. Introduction

The significance of exchanges of momentum, heat, water vapor, and trace gases such as CO_2 and CH_4 between the earth's surface and the atmospheric boundary layer (ABL) is rarely questioned (Brutsaert 1982; Stull 1988; Baldocchi et al. 2001; Stensrud 2007). These exchanges are governed by turbulence in the lower atmosphere, which is generated by both shear and buoyancy forces (Obukhov 1946; Monin and Obukhov 1954). It is often assumed that the turbulent transport of heat (as well as other scalars, such as water vapor and CO_2) is similar to the turbulent transport of momentum, given that the same eddies are the transporting agent for momentum, heat, and scalars. This assumption is often referred to as the Reynolds analogy (Kays 1994) and is used extensively in applications where eddy diffusivities are required. However, dissimilarity between turbulent transport of momentum and scalars for unstable stratification has been well documented in the ABL even prior to the weighty Kansas experiments (Businger et al. 1971; Brutsaert 2005).

Corresponding author address: Dan Li, Program in Atmospheric and Oceanic Sciences, Princeton University, 300 Forrestal Road, Sayre Hall, Princeton, NJ 08544.
E-mail: danl@princeton.edu

DOI: 10.1175/JAS-D-14-0335.1

The turbulent Prandtl number (Pr_t), a nondimensional number defined by the ratio of turbulent diffusivities of momentum and heat (Kays 1994), is commonly used to account for such dissimilarity. It is an important parameter in closure schemes for the Reynolds-averaged Navier–Stokes equations (Mellor and Yamada 1974; Stull 1988) and a similar parameter (i.e., the subgrid-scale Prandtl number) is also widely used in large-eddy simulation (LES) (Lilly 1992; Bou-Zeid et al. 2008). Numerous studies have reported Pr_t in wall-bounded turbulent boundary layers under ''ideal'' laboratory conditions (Yakhot et al. 1987; Kays 1994) and are not reviewed here. In the logarithmic region, where the Pr_t is expected to be a constant for fluids with molecular Prandtl number (Pr_m, the ratio of kinematic viscosity and molecular thermal diffusivity) of order unity such as air and water, the value of Pr_t reported in the literature ranges from 0.73 to 0.92 (Kays 1994). The Pr_t values reported in the well-studied atmospheric surface layer (ASL), which is the lowest 50–100 m of the ABL and corresponds to the logarithmic region reported in laboratory experiments (Businger et al. 1971; Högström 1988), exhibit much larger scatter even for near-neutral conditions (i.e., in the absence of buoyancy flux at the surface). Moreover, Pr_t in the ASL is further affected by the thermal stratification or atmospheric stability (Businger et al. 1971; Högström 1988; Li and Bou-Zeid 2011; Li et al. 2012). Explaining the causes of variability in the turbulent Prandtl number frames the scope of this work.

Despite significant advances in experiments and numerical simulations, a unified phenomenological theory that (i) elucidates possible departures of Pr_t from unity under near-neutral conditions, (ii) predicts variations of Pr_t with atmospheric stability from unstable through stable stratification in the ASL, and (iii) captures the impacts of various physical processes, such as flux transport terms, on Pr_t is currently lacking. Few recent studies (Katul et al. 2011; Li et al. 2012) have attempted to unravel the impact of thermal stratification on Pr_t in the ASL building on recent phenomenological arguments developed for the mean velocity profile in pipes (Gioia et al. 2010). In those studies, it was conjectured that the quasi-universal behavior of Pr_t with atmospheric stability parameters in the ASL may be connected to the quasi-universal spectral shapes whose finescales are reasonably described by Kolmogorov's theory in the inertial subrange (Katul et al. 2011; Li et al. 2012). Two recent studies formalized these linkages by analytically solving cospectral budgets for momentum and heat fluxes with prescribed idealized spectral shapes for vertical velocity and air temperature anchored to Kolmogorov's phenomenological theory at small scales (Katul et al. 2013b, 2014). The cospectral budgets method was shown to reproduce many bulk relations reported in experiments, simulations, and other models (Yamada 1975; Zilitinkevich et al. 2008, 2013), including the variation of Pr_t with atmospheric stability parameters. These studies suggest that linkages must exist between the spectral shapes of vertical velocity and air temperature and the bulk relations for the mean flow, which are principally determined from dimensional considerations or similarity theories.

Building on these phenomenological studies, the objective of this work is to generalize earlier phenomenological theories so that they can accommodate measured alterations in scaling laws in vertical velocity and air temperature spectra as atmospheric stability changes (Kader and Yaglom 1991). The dependence of Pr_t on other important physical processes that have not been considered in previous studies is also analyzed over a wide range of atmospheric stability conditions. The work here aims to link the spectral shapes of vertical velocity and air temperature, which describe the microscale states of turbulent kinetic and potential energy distributions, as shall be seen later, to the bulk flow properties, such as Pr_t. This linkage is particularly important for improving atmospheric modeling, because turbulence in the ABL spans an enormous range of scales, and different physical processes occur at different scales, which cannot be fully captured by parameterizations of bulk flow properties that are widely used in current numerical weather and climate models (Stensrud 2007). For example, there is strong coupling between small-scale turbulence and microphysical/aerosol processes (Bodenschatz et al. 2010). Moreover, the fast degeneration of small-scale turbulence but the long lifetime of large-scale turbulence after sunset is a key for maintaining turbulent mixing during nighttime in the ABL (Stull 1988).

The paper is organized as follows. Section 2 presents the theory, including the cospectral budgets for momentum and heat fluxes and how they are solved with the aid of idealized spectral shapes for vertical velocity and air temperature. Section 3 presents the resulting solution and compares the solution to experiments and other models, and section 4 concludes with the implications of these results to ASL flows.

2. Theory

a. Background and definitions

The turbulent Prandtl number is defined as (Kays 1994)

$$\mathrm{Pr}_t = \frac{K_m}{K_h} = \frac{-\overline{u'w'}/S}{-\overline{w'T'}/\Gamma}, \tag{1}$$

where K_m and K_h are turbulent or eddy diffusivities for momentum and heat, respectively; the overbar denotes averaging over coordinates of statistical homogeneity; u', w', and T' are turbulent fluctuations of the longitudinal velocity, vertical velocity, and air temperature, respectively, from their averages; $\overline{u'w'}$ is the turbulent momentum flux; $\overline{w'T'}$ is the turbulent sensible heat flux; $S = \partial\overline{U}(z)/\partial z$ is the mean velocity gradient; and $\Gamma = \partial\overline{T}(z)/\partial z$ is the mean air temperature gradient. To describe thermal stratification effects on S and Γ as well as other flow statistics, Monin–Obukhov similarity theory (MOST), is commonly employed (Obukhov 1946; Monin and Obukhov 1954; Businger and Yaglom 1971). MOST assumes that the flow in the ASL is stationary, planar homogeneous, and without subsidence, characterized by sufficiently high Reynolds and Peclet numbers so that viscous and molecular diffusion effects are negligible compared to K_m and K_h. When these assumptions are applied to the mean momentum and mean temperature budgets, the resulting outcome is that $\overline{u'w'}$ and $\overline{w'T'}$ become independent of height z. It is for this reason that the idealized ASL is also labeled as the constant-flux region. Using only dimensional considerations, Monin and Obukhov showed that distortions to the classical logarithmic velocity and air temperature profiles by buoyancy can be accounted for by stability correction functions ϕ_m and ϕ_h (Obukhov 1946; Monin and Obukhov 1954; Businger and Yaglom 1971), respectively, given as follows:

$$\phi_m(\zeta) = \frac{\kappa z}{u_*} S \quad \text{and} \tag{2}$$

$$\phi_h(\zeta) = \frac{\kappa z}{T_*} \Gamma, \tag{3}$$

where $\kappa \approx 0.4$ is the von Kármán constant, z is height from the ground surface or zero-plane displacement and is assumed to be much larger than the depth of the viscous sublayer, $u_* = (-\overline{u'w'})^{1/2}$ is the friction velocity, and $T_* = -\overline{w'T'}/u_*$ is a temperature scaling parameter. The stability parameter is defined as $\zeta = z/L$, with $L = -u_*^3/(\kappa\beta\overline{w'T'_v})$ being the Obukhov length (Obukhov 1946); $\beta = g/T_v$ is the buoyancy parameter; g is the gravitational acceleration; and T_v is the virtual temperature, with T_v^{-1} being the coefficient of expansion for an ideal gas. For simplicity, the virtual temperature is approximated by the air temperature here given the minor impact water vapor flux has on the overall buoyancy flux. When $\zeta < 0$, the ASL is unstable (e.g., during daytime over land); and when $\zeta > 0$, the ASL is stable (e.g., during nighttime over land). When $\zeta \approx 0$, the ASL is labeled as neutrally buoyant (or neutral), and no significant density gradients are expected due to surface heating or cooling.

Based on these definitions, Pr_t can be related to the stability correction functions using

$$\mathrm{Pr}_t = \frac{\phi_h(\zeta)}{\phi_m(\zeta)}. \tag{4}$$

b. Cospectral budgets of momentum and heat fluxes

The turbulent momentum and heat fluxes are linked to eddy sizes or wavenumbers using the cospectral definitions:

$$\overline{u'w'} = \int_0^\infty F_{uw}(K)\, dK \quad \text{and} \tag{5}$$

$$\overline{w'T'} = \int_0^\infty F_{wT}(K)\, dK, \tag{6}$$

where $F_{uw}(K)$ is the cospectrum of u' and w'; $F_{wT}(K)$ is the cospectrum of w' and T'; and K is a one-dimensional wavenumber in the streamwise direction. This definition of K is selected here to be consistent with the myriad of ASL experiments (Kaimal et al. 1972; Kaimal 1973; Kaimal and Finnigan 1994; Wyngaard and Cote 1972) that report spectra and cospectra from single-point time series measurements converted to one-dimensional streamwise wavenumber using Taylor's frozen turbulence hypothesis (Taylor 1938).

Before the cospectral budgets of momentum and sensible heat fluxes are presented, a brief summary of the main budgets of momentum and heat fluxes in the idealized ASL is provided. These budgets are

$$\frac{\partial\overline{u'w'}}{\partial t} = 0 = -\overline{w'w'}S - \frac{\partial\overline{w'w'u'}}{\partial z} - \frac{1}{\rho}\overline{u'\frac{\partial p'}{\partial z}} + \beta\overline{u'T'} - 2\nu\overline{\frac{\partial u'}{\partial z}\frac{\partial w'}{\partial z}} \quad \text{and} \tag{7}$$

$$\frac{\partial\overline{w'T'}}{\partial t} = 0 = -\overline{w'w'}\Gamma - \frac{\partial\overline{w'w'T'}}{\partial z} - \frac{1}{\rho}\overline{T'\frac{\partial p'}{\partial z}} + \beta\overline{T'T'} - (\nu + D_m)\overline{\frac{\partial w'}{\partial z}\frac{\partial T'}{\partial z}}, \tag{8}$$

where ρ is the mean air density, p is the air pressure, ν is the kinematic viscosity, and D_m is the molecular thermal diffusivity. The molecular Prandtl number of air is defined as $\mathrm{Pr}_m = \nu/D_m \approx 0.72$. The terms on the left-hand side of the equations represent changes in covariances (i.e., $\overline{u'w'}$ and $\overline{w'T'}$) with time. The terms on the right-hand side of the equations represent (in order): production terms due to the presence of mean velocity and air temperature gradients ($-\overline{w'w'}S$ and $-\overline{w'w'}\Gamma$), flux transport terms that represent turbulent transport of momentum and heat fluxes ($-\partial\overline{w'w'u'}/\partial z$ and

$-\partial\overline{w'w'T'}/\partial z$), pressure decorrelation terms due to interactions between pressure and velocity $[-(1/\rho)\overline{u'(\partial p'/\partial z)}]$ and between pressure and temperature $[-(1/\rho)\overline{T'(\partial p'/\partial z)}]$, buoyancy terms arising from thermal stratification in the ASL ($\beta\overline{u'T'}$ and $\beta\overline{T'T'}$), and molecular destruction terms $[-2\nu\overline{(\partial u'/\partial z)(\partial w'/\partial z)}$ and $-(\nu + D_m)\overline{(\partial w'/\partial z)(\partial T'/\partial z)}]$.

In correspondence, the cospectral budgets of momentum and heat fluxes in the ASL can be simplified as follows (Panchev 1971; Bos et al. 2004; Bos and Bertoglio 2007; Canuto et al. 2008; Katul et al. 2013a):

$$\frac{\partial F_{uw}(K)}{\partial t} = 0 = P_{uw}(K) + T_{uw}(K) + \pi_u(K) + \beta F_{uT}(K) - 2\nu K^2 F_{uw}(K) \quad \text{and} \tag{9}$$

$$\frac{\partial F_{wT}(K)}{\partial t} = 0 = P_{wT}(K) + T_{wT}(K) + \pi_T(K) + \beta F_{TT}(K) - (\nu + D_m)K^2 F_{wT}(K). \tag{10}$$

The terms on the left-hand side of the equations represent temporal changes in the cospectra. The terms on the right-hand side of the equations represent (in order): production P, flux transfer T, pressure decorrelation π, buoyancy (βF_{uT} and βF_{TT}), and molecular destruction. The term F_{uT} is the cospectrum of u' and T', and $F_{TT}(K)$ is the spectrum of air temperature. The molecular destruction terms are assumed to be small since they are, in principle, significant at sufficiently large wavenumber on the order of $1/\eta$, where η is the Kolmogorov microscale scale (on the order of 0.1–1 mm in the ASL). This is essentially assuming that eddies with sizes on the order of η do not contribute significantly to momentum and heat fluxes (at least when compared to other mechanisms such as π). The term $F_{uT}(K)$ is assumed to be small compared to $P_{uw}(K)$ and can be ignored. This is because it involves the correlation between the turbulent longitudinal velocity and air temperature, which is often small in the ASL, as demonstrated using direct numerical simulations (DNS) (Katul et al. 2014; Shah and Bou-Zeid 2014) and scaling arguments (Stull 1988). Hence, as a starting point, the cospectral budgets of momentum and heat fluxes here involve only the most basic terms common to all models and are given by

$$P_{uw}(K) + T_{uw}(K) + \pi_u(K) = 0 \quad \text{and} \tag{11}$$

$$P_{wT}(K) + T_{wT}(K) + \pi_T(K) + \beta F_{TT}(K) = 0. \tag{12}$$

The production terms can be obtained from direct Fourier transforming $-\overline{w'w'}S$ and $-\overline{w'w'}\Gamma$:

$$P_{uw}(K) = -F_{ww}(K)S \quad \text{and} \tag{13}$$

$$P_{wT}(K) = -F_{ww}(K)\Gamma, \tag{14}$$

where $F_{ww}(K)$ is the vertical velocity spectrum.

The flux transfer terms act to transport fluxes away from the peak of the cospectra; hence, they are parameterized using a spectral gradient diffusion model as follows (Bos et al. 2004; Bos and Bertoglio 2007):

$$T_{uw}(K) = -A_{UU}\frac{\partial}{\partial K}[\varepsilon^{1/3}K^{5/3}F_{uw}(K)] \quad \text{and} \tag{15}$$

$$T_{wT}(K) = -A_{TT}\frac{\partial}{\partial K}[\varepsilon^{1/3}K^{5/3}F_{wT}(K)], \tag{16}$$

where A_{UU} and A_{TT} are model constants associated with the flux transfer terms and ε is the mean dissipation rate of the turbulent kinetic energy (TKE). Throughout, the term "flux transport" is used in the context of Reynolds-averaged equation, while the term "flux transfer" is used in spectral space. It is also conceivable that the flux transport terms are negligible in an idealized ASL, but the flux transfer terms can be significant at a given K.

To model the pressure decorrelation terms, a Rotta-type parameterization is invoked in the spectral domain and corresponds to the one widely used in second-order closure schemes (Mellor and Yamada 1974; Yamada 1975). The limitations of such a Rotta approach are reasonably established (Choi and Lumley 2001); however, this parameterization remains the primary "work horse" model to close pressure-scalar and pressure-velocity covariances with some success (Launder et al. 1975). The following standard closure formulations are employed here (Launder et al. 1975; Pope 2000):

$$\pi_u(K) = -A_U\frac{F_{uw}(K)}{\tau_{uw}(K)} - C_{IU}P_{uw}(K) \quad \text{and} \tag{17}$$

$$\pi_T(K) = -A_T\frac{F_{wT}(K)}{\tau_{wT}(K)} - C_{IT}P_{wT}(K), \tag{18}$$

where A_T and A_U ($\approx$1.8) are the Rotta constants (Pope 2000), C_{IT} and C_{IU} ($\approx$3/5) are constants associated with isotropization of production terms (herein referred to as the isotropization constants), which can be determined using rapid distortion theory in homogeneous turbulence (Pope 2000). The parameters $\tau_{uw}(K)$ and $\tau_{wT}(K)$ are relaxation time scales for momentum and heat fluxes, respectively, which are also wavenumber dependent. A widely used formulation for $\tau_{uw}(K)$ and $\tau_{wT}(K)$ is given by the following (Corrsin 1961; Bos et al. 2004; Bos and Bertoglio 2007; Cava and Katul 2012; Katul et al. 2014):

$$\tau_{uw}(K) = \tau_{wT}(K) = \varepsilon^{-1/3}K^{-2/3}. \tag{19}$$

With these parameterizations, Eqs. (11) and (12) reduce to

$$\frac{\partial F_{uw}(K)}{\partial K}+\left(\frac{A_U}{A_{UU}}+\frac{5}{3}\right)K^{-1}F_{uw}(K)$$
$$=-\frac{(1-C_{IU})S}{A_{UU}\varepsilon^{1/3}}F_{ww}(K)K^{-5/3} \quad \text{and} \qquad (20)$$

$$\frac{\partial F_{wT}(K)}{\partial K}+\left(\frac{A_T}{A_{TT}}+\frac{5}{3}\right)K^{-1}F_{wT}(K)$$
$$=-\frac{(1-C_{IT})\Gamma}{A_{TT}\epsilon^{1/3}}F_{ww}(K)K^{-5/3}$$
$$+\frac{\beta}{A_{TT}\varepsilon^{1/3}}F_{TT}(K)K^{-5/3}. \qquad (21)$$

The above equations for $F_{uw}(K)$ and $F_{wT}(K)$ can be solved once $F_{ww}(K)$ and $F_{TT}(K)$ are known or specified. The precise spectral shapes of $F_{ww}(K)$ and $F_{TT}(K)$ will be discussed later. However, for illustration purposes, it is convenient to begin with a single power-law formulation with $F_{ww}(K)=C_{ww}K^{-\alpha}$ and $F_{TT}(K)=C_{TT}K^{-\gamma}$, where α and γ are spectral scaling exponents and C_{ww} and C_{TT} are normalization factors.

c. *Solving the cospectral budgets for momentum and heat fluxes*

Equations (20) and (21) reduce to two (uncoupled) first-order ordinary differential equations, given as follows:

$$\frac{dF_{uw}(K)}{dK}+D_1K^{-1}F_{uw}(K)=D_2C_{ww}K^{-\alpha-5/3} \quad \text{and} \qquad (22)$$

$$\frac{dF_{wT}(K)}{dK}+D_3K^{-1}F_{wT}(K)=D_4C_{ww}K^{-\alpha-5/3}$$
$$+D_5C_{TT}K^{-\gamma-5/3}, \qquad (23)$$

where $D_1=A_U/A_{UU}+5/3$, $D_2=-(1-C_{IU})S/(A_{UU}\varepsilon^{1/3})$, $D_3=A_T/A_{TT}+5/3$, $D_4=-(1-C_{IT})\Gamma/(A_{TT}\varepsilon^{1/3})$, and $D_5=\beta/(A_{TT}\varepsilon^{1/3})$. These two equations can be solved to yield the following:

$$F_{uw}(K)=\frac{D_2}{-\alpha-2/3+D_1}C_{ww}K^{-\alpha-2/3}+E_1K^{-D_1} \quad \text{and} \qquad (24)$$

$$F_{wT}(K)=\frac{D_4}{-\alpha-2/3+D_3}C_{ww}K^{-\alpha-2/3}$$
$$+\frac{D_5}{-\gamma-2/3+D_3}C_{TT}K^{-\gamma-2/3}+E_2K^{-D_3}, \qquad (25)$$

where E_1 and E_2 are integration constants to be determined later. The above solutions implicitly require $D_1\geq\alpha+2/3$ and $D_3\geq\max(\alpha+2/3,\ \gamma+2/3)$. That is, $A_U/A_{UU}\geq\alpha-1$, and $A_T/A_{TT}\geq\max(\alpha-1,\ \gamma-1)$.

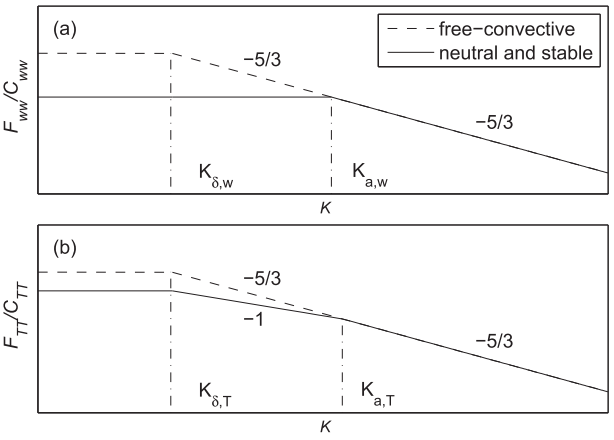

FIG. 1. The assumed shapes of (a) the vertical velocity and (b) the air temperature spectra as a function of wavenumber K for near-neutral and stable conditions (solid lines) and free-convective conditions (dashed lines). When $K>K_a$, the spectra under near-neutral and free-convective conditions overlap. The transition wavenumbers K_δ and K_a are indicated by the dashed–dotted lines, and they can be different for $F_{ww}(K)$ and $F_{TT}(K)$, as denoted by the subscripts w and T, respectively.

d. *Idealized spectral shapes of $F_{ww}(K)$ and $F_{TT}(K)$*

In this section, multiexponent approximations to $F_{ww}(K)$ and $F_{TT}(K)$ are evaluated so that Eqs. (24) and (25) can be integrated across all K so as to obtain the momentum and heat fluxes. One plausible approximation assumes that the spectra of vertical velocity and temperature simply follow the Kolmogorov $-5/3$ scaling for all $K>K_a$ and level off for all $K<K_a$ for near-neutral and stable stratification, where $K_a\approx 1/z$ is a transition wavenumber delineating attached eddies to the boundary from detached eddies assumed to follow inertial subrange scaling (Katul et al. 2014). An outcome of this approximation is a connection between A_U, C_{IU}, the Kolmogorov phenomenological constant C_o in the inertial subrange, and the von Kármán constant κ (Katul et al. 2014). Later, this idealized spectral shape of $F_{TT}(K)$ was modified in Li et al. (2015, manuscript submitted to *Bound.-Layer Meteor.*) to accommodate the presence of -1 scaling in the low-wavenumber part based on ASL measurements above lakes and glaciers. Both studies (Katul et al. 2014; Li et al. 2015, manuscript submitted to *Bound.-Layer Meteor.*) focused on stable ASL conditions and did not consider any effects of flux transfer terms in their analyses. Other studies did consider flux transfer terms in their scalar cospectral budgets (Cava and Katul 2012; Katul et al. 2013a), but these studies primarily focused on the effects of flux transfer terms on inertial subrange scales, not on bulk flow properties.

More realistic spectral shapes are assumed here for both $F_{ww}(K)$ and $F_{TT}(K)$, shown in Fig. 1, that reflect observed scaling exponents in the ASL reported from long-term field experiments (Kader and Yaglom 1991).

Both $F_{ww}(K)$ and $F_{TT}(K)$ follow the expected Kolmogorov $-5/3$ power-law scaling at sufficiently large wavenumber (Kolmogorov 1941). The $-5/3$ scaling commences from K_δ under free-convective conditions ($\zeta \to -\infty$) but starts from $K_a \approx 1/z$ under neutral and stable conditions. A -1 power-law scaling is allowed to exist over a range of low wavenumbers (from K_δ to K_a) for $F_{TT}(K)$, but not for $F_{ww}(K)$ under near-neutral and stable conditions to explore the impact of the possible occurrence of a -1 scaling in $F_{TT}(K)$, as suggested by several ASL experiments reported elsewhere (Kader and Yaglom 1991; Katul et al. 1995; Katul and Chu 1998; Li et al. 2015, manuscript submitted to *Bound.-Layer Meteor.*). Both spectra are assumed to become invariant with K when $K < K_\delta$ to accommodate finite energy associated with very-large-scale and super structures recently reported in laboratory and ASL turbulence (Guala et al. 2010; Hutchins et al. 2012) and reviewed elsewhere (Marusic et al. 2010; Smits et al. 2011). Hence, as a compromise between realistic spectral shapes in the ASL and the need for maximum simplicity in analytical tractability, the following idealized forms for $F_{ww}(K)$ and $F_{TT}(K)$ are assumed:

$$F_{ww}(K) = \begin{cases} C_{ww_1} K^{-\alpha_1}, & \text{for} \quad K < K_{\delta,w} \\ C_{ww_2} K^{-\alpha_2}, & \text{for} \quad K_{\delta,w} < K < K_{a,w} \\ C_{ww_3} K^{-\alpha_3}, & \text{for} \quad K > K_{a,w} \end{cases} \quad \text{and}$$

$$F_{TT}(K) = \begin{cases} C_{TT_1} K^{-\gamma_1}, & \text{for} \quad K < K_{\delta,T} \\ C_{TT_2} K^{-\gamma_2}, & \text{for} \quad K_{\delta,T} < K < K_{a,T} \\ C_{TT_3} K^{-\gamma_3}, & \text{for} \quad K > K_{a,T} \end{cases}$$

As can be seen from Fig. 1, $\alpha_1 = 0$, $\gamma_1 = 0$, and $\alpha_3 = \gamma_3 = 5/3$. Under neutral and stable conditions, $\alpha_2 = 0$ and $\gamma_2 = 1$, while $\alpha_2 = \gamma_2 = 5/3$ under free-convective conditions. An interpolation $\alpha_2 = 5/3[1 - \exp(5\zeta)]$ is used to cover the whole range of $\zeta \le 0$ so that α_2 satisfies both the neutral and the free-convective limits. Similarly, $\gamma_2 = 2/3[1 - \exp(5\zeta)] + 1$ is used when $\zeta \le 0$. As such, the possible existence of -1 exponent in air temperature spectra is restricted to be within a limited range of ζ (i.e., under near-neutral conditions) when $\zeta < 0$, as reported in previous ASL experiments (Kader and Yaglom 1991; Katul et al. 1995).

The values of C_{ww_3} and C_{TT_3} can be determined from Kolmogorov's theory (Kolmogorov 1941) for the inertial subrange: $C_{ww_3} = C_o \varepsilon^{2/3}$ and $C_{TT_3} = C_T N_T \varepsilon^{-1/3}$, where C_o is defined above and C_T is the Kolmogorov–Obukhov–Corrsin phenomenological constant. For a one-dimensional-wavenumber interpretation, their values are $C_o = 0.65$ and $C_T = 0.8$ (Ishihara et al. 2002; Chung and Matheou 2012). The parameter ε is the mean turbulent kinetic energy dissipation rate, and N_T is the mean temperature variance dissipation rate. The values of C_{ww_2}, C_{ww_1}, C_{TT_2}, and C_{TT_1} are then determined from continuity constraints on the spectra (e.g., $C_{ww_3} K_{a,w}^{-\alpha_3} = C_{ww_2} K_{a,w}^{-\alpha_2}$ and $C_{ww_2} K_{\delta,w}^{-\alpha_2} = C_{ww_1} K_{\delta,w}^{-\alpha_1}$).

It is to be noted that the turbulent kinetic energy in the vertical direction (TKE_w) and the turbulent potential energy (TPE) can be linked to $F_{ww}(K)$ and $F_{TT}(K)$ (Zilitinkevich et al. 2007, 2008, 2013; Li et al. 2015, manuscript submitted to *Bound.-Layer Meteor.*) using

$$\mathrm{TKE}_w = \frac{1}{2} \int_0^\infty F_{ww}(K)\, dK \quad \text{and} \tag{26}$$

$$\mathrm{TPE} = \frac{1}{2} \frac{\beta^2}{N^2} \int_0^\infty F_{TT}(K)\, dK. \tag{27}$$

Hence, specifying $F_{ww}(K)$ and $F_{TT}(K)$ is analogous to specifying the vertical kinetic and potential energy distributions of turbulent eddies at each K. This provides a clear connection between the proposed cospectral budget model here and the energy- and flux-budget (EFB) turbulence closure approach proposed by Zilitinkevich et al. (2007, 2008, 2013), since TKE_w/TPE was shown to be a significant parameter in the EFB model.

e. The integration constants E_1 and E_2

Besides the spectral shapes of $F_{ww}(K)$ and $F_{TT}(K)$, the integration constants (i.e., E_1 and E_2) are also required to evaluate $F_{uw}(K)$ and $F_{wT}(K)$. Katul et al. (2013a) assumed that $\partial F_{wT}(K)/\partial K$ becomes zero when $K = K_a$. As a result, the flux transfer term in the cospectral budget of heat flux affects ϕ_h only by a constant that is dependent on A_{TT}/A_T. In our study, the integration constants (i.e., E_1 and E_2) are simply assumed to be zero. This is supported by experiments and DNS that reported $-7/3$ power-law scalings in the inertial subrange of momentum and heat flux cospectra (Kaimal and Finnigan 1994; Pope 2000). Note, Eqs. (24) and (25) yield $-7/3$ scaling in the inertial subrange of $F_{uw}(K)$ and $F_{wT}(K)$, respectively, when $E_1 = 0$ and $E_2 = 0$ are assumed, given $\alpha = 5/3$ and $\gamma = 5/3$ in the inertial subrange. It is pointed out here that the impact of flux transfer terms is not completely eliminated by doing so since the other terms on the right-hand side of Eqs. (24) and (25) are still affected by flux transfer terms. However, the impact of the flux transfer terms on the anomalous scalings in the inertial subrange of momentum and heat flux cospectra are excluded when setting $E_1 = 0$ and $E_2 = 0$.

3. Results

Using the idealized spectral shapes of $F_{ww}(K)$ and $F_{TT}(K)$ and the assumption of $E_1 = E_2 = 0$, Eqs. (5) and (6) can now be evaluated:

$$\overline{u'w'} = \int_0^\infty F_{uw}(K)\,dK = f_1 D_2 C_o \varepsilon^{2/3} \quad \text{and} \tag{28}$$

$$\overline{w'T'} = \int_0^\infty F_{wT}(K)\,dK = g_1 D_4 C_o \varepsilon^{2/3} + g_2 D_5 C_T N_T \varepsilon^{-1/3} = g_1 D_4 C_o \varepsilon^{2/3} Q. \tag{29}$$

Again, for maximum simplicity, local balances between production and dissipation terms in the TKE and in the temperature variance budgets are assumed to yield (Katul et al. 2014; Li et al. 2015, manuscript submitted to *Bound.-Layer Meteor.*):

$$\mathrm{Pr}_t = \frac{-\overline{u'w'}/S}{-\overline{w'T'}/\Gamma} = \frac{A_{TT}(1-C_{IU})}{A_{UU}(1-C_{IT})}\frac{f_1}{g_1}\frac{1}{Q}, \tag{30}$$

where

$$Q = 1 - \frac{1}{1-C_{IT}}\frac{C_T}{C_o}\frac{g_2}{g_1}\frac{\zeta}{(\phi_m - \zeta)}, \tag{31}$$

$$f_1 = \frac{1}{(-\alpha_1 - 2/3 + D_1)(-\alpha_1 + 1/3)} K_{\delta,w}^{-\alpha_2+1/3} K_{a,w}^{\alpha_2-\alpha_3} + \frac{1}{(-\alpha_2 - 2/3 + D_1)(-\alpha_2 + 1/3)}\left(K_{a,w}^{-\alpha_3+1/3} - K_{\delta,w}^{-\alpha_2+1/3} K_{a,w}^{\alpha_2-\alpha_3}\right) + \frac{1}{(-\alpha_3 - 2/3 + D_1)(-\alpha_3 + 1/3)}\left(-K_{a,w}^{-\alpha_3+1/3}\right), \tag{32}$$

$$g_1 = \frac{1}{(-\alpha_1 - 2/3 + D_3)(-\alpha_1 + 1/3)} K_{\delta,w}^{-\alpha_2+1/3} K_{a,w}^{\alpha_2-\alpha_3} + \frac{1}{(-\alpha_2 - 2/3 + D_3)(-\alpha_2 + 1/3)}\left(K_{a,w}^{-\alpha_3+1/3} - K_{\delta,w}^{-\alpha_2+1/3} K_{a,w}^{\alpha_2-\alpha_3}\right) + \frac{1}{(-\alpha_3 - 2/3 + D_3)(-\alpha_3 + 1/3)}\left(-K_{a,w}^{-\alpha_3+1/3}\right), \quad \text{and} \tag{33}$$

$$g_2 = \frac{1}{(-\gamma_1 - 2/3 + D_3)(-\gamma_1 + 1/3)} K_{\delta,T}^{-\gamma_2+1/3} K_{a,T}^{\gamma_2-\gamma_3} + \frac{1}{(-\gamma_2 - 2/3 + D_3)(-\gamma_2 + 1/3)}\left(K_{a,T}^{-\gamma_3+1/3} - K_{\delta,T}^{-\gamma_2+1/3} K_{a,T}^{\gamma_2-\gamma_3}\right) + \frac{1}{(-\gamma_3 - 2/3 + D_3)(-\gamma_3 + 1/3)}\left(-K_{a,T}^{-\gamma_3+1/3}\right). \tag{34}$$

To ensure a downgradient sensible heat flux, $Q > 0$. The parameters f_1, g_1, and g_2 encode the shape functions of the vertical velocity and temperature spectra. When $\zeta = 0$ (i.e., under neutral conditions), Pr_t (denoted as $\mathrm{Pr}_{t,\mathrm{neu}}$) becomes

$$\mathrm{Pr}_{t,\mathrm{neu}} = \frac{A_{TT}(1-C_{IU})}{A_{UU}(1-C_{IT})}\frac{f_1}{g_1}. \tag{35}$$

The departure of $\mathrm{Pr}_{t,\mathrm{neu}}$ from unity, as predicted from earlier theories (Mellor and Yamada 1974; Yamada 1975; Reynolds 1975; Yakhot et al. 1987; Zilitinkevich et al. 2008, 2013) and many experiments and simulations (Businger et al. 1971; Högström 1988; Kays 1994) can now be critically examined. The main mechanisms that introduce such departures are $A_{TT} \neq A_{UU}$, $C_{IU} \neq C_{IT}$, and $f_1 \neq g_1$. As shown later, inequality between f_1 and g_1 is primarily due to the inequality between A_{TT}/A_T and A_{UU}/A_U. Consequently, inequality in the Rotta constants, isotropization constants, and constants in flux transfer terms between momentum and heat lead to $\mathrm{Pr}_{t,\mathrm{neu}}$ different from unity. Naturally, the assumed balances between production and dissipation in the turbulent kinetic energy and temperature variance budgets also introduce further uncertainties. The evidence in the literature thus far seems to be in support of such approximations for unstable conditions when data are conditioned for stationarity and planar homogeneity in the absence of subsidence (Hsieh and Katul 1997; Charuchittipan and Wilson 2009; Salesky et al. 2013), but for stable conditions, the emerging picture is far less clear (Salesky et al. 2013). Moreover, most ASL data tend to be infected by high-intensity turbulent flow conditions at the very stable and near-convective conditions, thereby complicating the use of Taylor's frozen turbulence hypothesis to infer dissipation rates from structure functions or spectra.

From Eq. (30), Pr_t can also be expressed as $\mathrm{Pr}_t^{-1} = \mathrm{Pr}_{t,\mathrm{neu}}^{-1} Q$, where Q represents the additional effects of

stability on the turbulent Prandtl number separate from those expected in near-neutral conditions. Denoting $\omega_1 = [1/(1 - C_{IT})](C_T/C_o)(g_2/g_1)$, Eq. (30) is recast as follows:

$$\mathrm{Pr}_t^{-1} = \mathrm{Pr}_{t,\mathrm{neu}}^{-1}\left[1 - \omega_1 \frac{\zeta}{(\phi_m - \zeta)}\right]. \tag{36}$$

Assuming that the stability correction function ϕ_m is given by its Businger–Dyer form (Businger et al. 1971), a form shown to be reasonable from recent multilevel ASL experiments (Salesky et al. 2013), the dependence of Pr_t on ζ is then primarily controlled by ω_1: namely, by the ratio of the Kolmogorov to the Kolmogorov–Obukhov–Corrsin phenomenological constants (C_T/C_O); a constant associated with isotropization of the production (C_{IT}), the value of which can be determined from rapid distortion theory in homogeneous turbulence (=3/5); and the ratio of g_2/g_1 encoding differences in the spectral shapes of vertical velocity and air temperature. The near-universal values of the Kolmogorov and the Kolmogorov–Obukhov–Corrsin phenomenological constants have been investigated extensively (Sreenivasan 1995, 1996; Yeung and Zhou 1997). The dependence of the Pr_t–ζ relation on the ratio of two constants suggests that a possible universal Pr_t–ζ relation (or Pr_t–R_g, where R_g is the gradient Richardson number; see below) may be inherited from the Kolmogorov cascade in the inertial subrange, which is consistent with recent literature demonstrating that there are strong linkages between macroscopic features in the logarithmic region of wall-bounded turbulent flows and the Kolmogorov scaling (Gioia et al. 2010; Katul et al. 2013a, 2014, 2013b; Li et al. 2012; Zúñiga Zamalloa et al. 2014; Katul and Manes 2014). In addition, the fact that the Pr_t–ζ relation depends on the ratio of C_T/C_O (basic constants associated with spectral shapes of temperature and velocity) suggests that both TPE and TKE_w are important energetics in the ASL, consistent with the EFB model (Zilitinkevich et al. 2007, 2008, 2013). To illustrate this point further, assuming the -1 scaling is absent in air temperature spectra under neutral and stable conditions (see Fig. 1), C_T/C_O is related to the ratio of TPE and TKE_w through

$$\frac{\mathrm{TPE}}{\mathrm{TKE}_w} = \frac{C_T}{C_o}\frac{R_f}{1 - R_f}. \tag{37}$$

Interestingly, R_f at which the vertical turbulent kinetic energy is balanced by the turbulent potential energy is $R_f = (1 + C_T/C_O)^{-1} \approx 0.45$. This constraint on $R_f(<0.45)$ is much stronger than R_f imposed from TKE balance considerations alone [i.e., $\varepsilon = -\overline{w'u'}S(1 - R_f) > 0$] that yield $R_f < 1$. However, this constraint on $R_f(<0.45)$ is not the most severe, as discussed next.

In addition to ζ, R_f and R_g are also widely used to indicate the thermal stratification or the stability effect in the ASL. Using $R_f = \zeta/\phi_m$, Pr_t can be formulated as a function of R_f:

$$\mathrm{Pr}_t^{-1} = \mathrm{Pr}_{t,\mathrm{neu}}^{-1}\left[1 - \omega_1 \frac{R_f}{(1 - R_f)}\right]. \tag{38}$$

Given that the $\mathrm{Pr}_t = R_g/R_f$, Pr_t can be readily expressed as a function of R_g, as follows:

$$\mathrm{Pr}_t^{-1} = \mathrm{Pr}_{t,\mathrm{neu}}^{-1}\left[\frac{1 + \omega_2 R_g - \sqrt{-4R_g + (-1 - \omega_2 R_g)^2}}{2R_g}\right], \tag{39}$$

where $\omega_2 = \omega_1 + 1$. The flux Richardson number is also readily related to R_g through

$$R_f = \mathrm{Pr}_{t,\mathrm{neu}}^{-1}\left[\frac{1 + \omega_2 R_g - \sqrt{-4R_g + (-1 - \omega_2 R_g)^2}}{2}\right]. \tag{40}$$

An interesting outcome of Eq. (40) is that R_f is limited by some threshold or the "maximum flux Richardson number" R_{fm} as R_g increases. The physical meaning of this maximum flux Richardson number is that R_f cannot increase infinitely under stable conditions as R_g increases (Galperin et al. 2007). The gradient Richardson number can be viewed as an external variable that characterizes the mean flow; as a result, the increase of R_g is not limited by the internal turbulence state (Zilitinkevich et al. 2007). However, R_f depends on the internal turbulence state and becomes saturated at high stability, as already shown in Katul et al. (2014). This maximum flux Richardson number can be inferred from Eq. (38), given that the sensible heat flux is downgradient (hence $Q > 0$ and $\mathrm{Pr}_t > 0$) and $R_f < 1$ so that

$$R_{fm} = \frac{1}{\omega_1 + 1} = \frac{1}{\omega_2}. \tag{41}$$

When $A_U = A_T = 1.8$, $C_{IU} = C_{IT} = 3/5$, and $g_2 = g_1$, the value of R_{fm} is 0.25, which is in agreement with the values of R_{fm} reported in the literature (0.2–0.25). It is pointed out here that R_{fm} should not be equated to the "critical gradient Richardson number" R_{gc} inferred from the classic Miles–Howard theory. This aforementioned

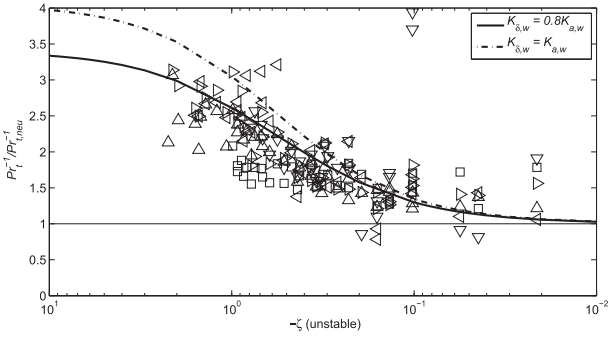

FIG. 2. Comparison between modeled $\mathrm{Pr}_t^{-1}/\mathrm{Pr}_{t,\mathrm{neu}}^{-1}$ from the cospectral budgets when $K_{\delta,T} = K_{a,T} = K_{a,w}$ (i.e., no -1 power scaling in the air temperature spectra) and $K_{\delta,w} = 0.8K_{a,w}$ (black solid line) or $K_{\delta,w} = K_{a,w}$ (black dashed line) with experiments and simulations for a wide range of unstable conditions. The inequality between $K_{\delta,w}$ and $K_{a,w}$ only affects the unstable part, since only under unstable conditions is the scaling between $K_{\delta,w}$ and $K_{a,w}$ nonzero. Data are from ASL field experiments ▷ in Kansas (Businger et al. 1971); ▽ in Kerang and Hay, Australia (Brutsaert 1982); ◁ in Pampa, Brazil (Moraes 2000); Δ in Tsimlyansk, Russia (Kader and Yaglom 1990); and □ in Gotland Island, Sweden (Smedman et al. 2007).

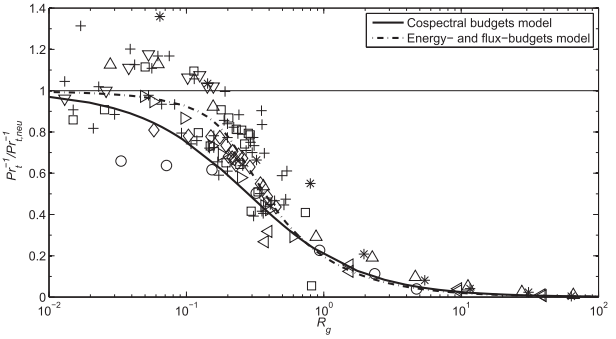

FIG. 3. Comparison between modeled $\mathrm{Pr}_t^{-1}/\mathrm{Pr}_{t,\mathrm{neu}}^{-1}$ from the cospectral budgets model and from the EFB model with experiments and simulations for a wide range of stable conditions. Data are from numerical simulations, including DNS and LES, laboratory, and field experiments: ▷ for DNS (Shih et al. 2000), ◁ for DNS (Stretch et al. 2010), ▽ for DNS (Chung and Matheou 2012), Δ for LES (Esau and Grachev 2007), ◇ for LES (Andren 1995), + for water channel (Rohr et al. 1988), □ for wind tunnel (Webster 1964), ○ for wind tunnel (Ohya 2001), and * for SHEBA field experiment (Grachev et al. 2007).

theory yields a prediction of a critical $R_g = 0.25$ associated with instability of a laminar boundary layer (Miles 1961; Howard 1961). The critical gradient Richardson number of the Miles–Howard theory was assumed to represent a critical Richardson number in some turbulent studies, though this representation has been questioned (Monin and Yaglom 1971). The concept of the critical gradient Richardson number characterizing a laminar–turbulent transition is not applicable to a laminarization of a turbulent ASL, as discussed elsewhere (Galperin et al. 2007; Zilitinkevich et al. 2007). Different from a critical gradient Richardson number of the Miles–Howard theory, the maximum flux Richardson number is used to indicate a saturation value of R_f with increasing R_g in turbulent flows. We note that R_{fm} has also been labeled as a ''critical'' Richardson number in some other studies (Yamada 1975; Grachev et al. 2013), but this label is not linked with the Miles–Howard theory (even though the maximum flux Richardson number value is close to 0.25). To avoid ambiguity in nomenclature, this saturated value in a turbulent ASL is labeled as the maximum flux Richardson number. The implications of this R_{fm} in the cospectral budget framework are explained later. In addition, how the value of R_{fm} is influenced by the possible existence of -1 scaling in air temperature spectra and the flux transfer terms are also explored.

a. *Evaluation of modeled* Pr_t *from proposed cospectral budgets*

Previous studies demonstrated the utility of the cospectral budgets in reproducing variations of $\mathrm{Pr}_t^{-1}/\mathrm{Pr}_{t,\mathrm{neu}}^{-1}$ for stable conditions when $g_2 = g_1$ (Katul et al. 2014). Figure 2 shows modeled $\mathrm{Pr}_t^{-1}/\mathrm{Pr}_{t,\mathrm{neu}}^{-1}$ or Q using the cospectral budgets when $K_{\delta,T} = K_{a,T}$ [i.e., the -1 power-law scaling is absent in $F_{TT}(K)$ at low K] for unstable conditions. Since the ratio of g_2/g_1 is also dependent on the inequality between $K_{\delta,w}$ and $K_{a,w}$ under unstable conditions, results with $K_{\delta,w} = K_{a,w}$ (the black dashed line) and $K_{\delta,w} = 0.8K_{a,w}$ (the black line) are both shown in Fig. 2. These predictions are compared to data from many field experiments. It is clear that the cospectral budgets method captures the general variation of $\mathrm{Pr}_t^{-1}/\mathrm{Pr}_{t,\mathrm{neu}}^{-1}$ with ζ under unstable conditions reported in many experiments. The model with $K_{\delta,w} = 0.8K_{a,w}$ (black line) reduces Pr_t under very unstable conditions and better agrees with experiments, suggesting the need for a further extension of the $-5/3$ scaling in $F_{ww}(K)$ as instability increases, which is in agreement with spectral shapes reported elsewhere for forced and free convection in the ASL (Kader and Yaglom 1991).

The cospectral budgets model is further compared against the EFB turbulence closure model developed for stable conditions (Zilitinkevich et al. 2007, 2008, 2013) in Fig. 3. The Pr_t–R_g relation instead of the Pr_t– ζ relation is examined under stable conditions to avoid self-correlation between Pr_t and ζ or R_f reported in the experiments (Klipp and Mahrt 2004; Esau and Grachev 2007; Grachev et al. 2007; Anderson 2009; Rodrigo and Anderson 2013). Zilitinkevich et al. (2013) pointed out that under stable conditions, Pr_t increases as R_g increases and has the asymptote $\mathrm{Pr}_t \to R_g/R_{fm}$ when $R_g \to \infty$. Figure 3 shows that the cospectral budgets model reproduces the increasing trend of Pr_t (or the

decreasing trend of Pr_t^{-1}) as R_g increases, which is also consistent with other theoretical work using the quasi-normal scale elimination theory (Galperin et al. 2007). Moreover, as $R_g \to \infty$, Pr_t is almost a linear function of R_g, the slope of which is also similar to the slope from the EFB model (not shown here but similar slopes in the two models can be inferred from Fig. 3), implying that the R_{fm} values are similar in both the cospectral budgets model and the EFB model. It is, however, noted here that $R_{fm} = 0.25$ was preset in the EFB model, while it is an outcome of model calculations in the cospectral budgets.

b. *The impact of possible −1 scaling in air temperature spectra on* Pr_t

The −1 power-law scaling has been reported in several ASL experiments for the spectra of streamwise velocity, pressure, and skin and air temperature, especially for near-neutral conditions (Kader and Yaglom 1991; Katul et al. 1995, 1996; Katul and Chu 1998; McNaughton and Laubach 2000; Katul et al. 2012; Banerjee and Katul 2013; Katul et al. 2013b). A recent study also showed that a −1 power-law scaling existed in air temperature spectra for near-neutral to mildly stable conditions over lakes and glaciers (Li et al. 2015, manuscript submitted to *Bound.-Layer Meteor.*). However, the universal character of the −1 scaling in air temperature spectra remains questionable. For example, early experiments by Pond and coworkers over sea do report a K^{-1} scaling in their longitudinal velocity spectra but not in their air temperature (or vertical velocity) spectra (Pond et al. 1966). Likewise, measured air temperature spectra in a stable ASL reported by Grachev et al. (2013) also do not support an extensive −1 power-law scaling. Hence, an exploration of how the −1 power-law scaling in air temperature spectra may modify Pr_t is warranted. The possible existence of −1 power law in the air temperature spectra can be represented here by the inequality between $K_{\delta,T}$ and $K_{a,T}$. As can be seen from Eqs. (35), (32), and (33), the possible existence of −1 scaling has no impact on the $\mathrm{Pr}_{t,\mathrm{neu}}$ but affects the ratio g_2/g_1 and, thus, Q. Figure 4 shows the variations of $\mathrm{Pr}_t^{-1}/\mathrm{Pr}_{t,\mathrm{neu}}^{-1}$ as functions of ζ, R_g, and R_f for three cases ($K_{\delta,T}/K_{a,T} = 1$, $K_{\delta,T}/K_{a,T} = 0.5$, and $K_{\delta,T}/K_{a,T} = 0.2$).

First, $\mathrm{Pr}_t^{-1}/\mathrm{Pr}_{t,\mathrm{neu}}^{-1}$ when $K_{\delta,T} = K_{a,T}$ is examined. It is clear that the $\mathrm{Pr}_t^{-1}/\mathrm{Pr}_{t,\mathrm{neu}}^{-1}$ increases as the atmosphere becomes more unstable, while it decreases as the atmosphere becomes more stable, implying that sensible heat is transferred more efficiently under unstable conditions and less efficiently under stable conditions when compared to momentum. The relation between $\mathrm{Pr}_t^{-1}/\mathrm{Pr}_{t,\mathrm{neu}}^{-1}$ and ζ is almost identical to that between $\mathrm{Pr}_t^{-1}/\mathrm{Pr}_{t,\mathrm{neu}}^{-1}$ and R_g, which is in agreement with Businger (1988) regarding a near correspondence between ζ and R_g. A difference is

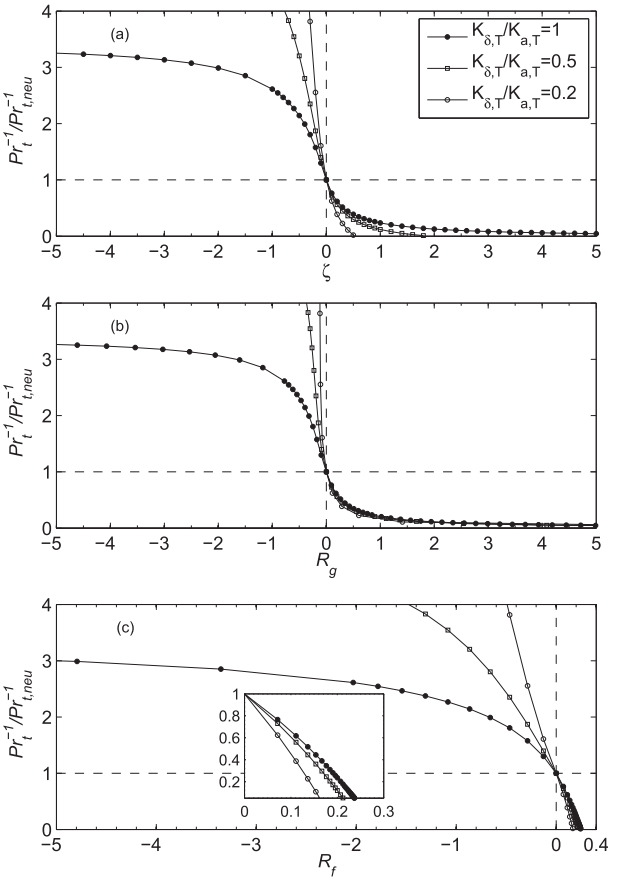

FIG. 4. $\mathrm{Pr}_t^{-1}/\mathrm{Pr}_{t,\mathrm{neu}}^{-1}$ as a function of (a) $\zeta = z/L$, (b) R_g, and (c) R_f when the −1 scaling law is prevalent in the spectra of air temperature. Here, $K_{\delta,T}$ can be smaller than $K_{a,T}$. The inset in (c) further emphasizes the results for stable ASL conditions. Note that $A_{TT}/A_T = 1$ is assumed here, but other values of A_{TT}/A_T yield similar results.

observed in the relation between Pr_t and R_f (Fig. 4c). Unlike ζ and R_g, which may increase to very large values under stable conditions, R_f is limited by R_{fm}. Again, the numerical value of this R_{fm} is a direct outcome of the cospectral budget model, as demonstrated by Eq. (41), which is also in agreement with the values of R_{fm} reported in the literature and assumed in the EFB model.

Figure 4 further shows how variations of $\mathrm{Pr}_t^{-1}/\mathrm{Pr}_{t,\mathrm{neu}}^{-1}$ with ζ, R_g, and R_f are modified by the possible existence of a −1 scaling in the air temperature spectra. To simplify the analysis, $A_{TT}/A_T = 1$ is assumed here; but, as shown later, the exact value of A_{TT}/A_T only changes the stability impact on $\mathrm{Pr}_t^{-1}/\mathrm{Pr}_{t,\mathrm{neu}}^{-1}$ in a minor way. It is clear that Pr_t^{-1} is increased significantly when $\zeta < 0$ but decreased when $\zeta > 0$ because of the possible existence of a −1 power-law scaling. This result implies that when such a −1 power-law scaling is primarily observed in the air temperature spectra, Pr_t becomes more sensitive to the atmospheric stability effect. This may be because of the existence of large-scale, inactive eddies under

such conditions (Katul et al. 1996; McNaughton and Brunet 2002), which cause −1 power-law scaling in the air temperature spectra and allow atmospheric stability to affect heat transport more effectively. As the extent of the −1 scaling increases (i.e., as $K_{\delta,T}/K_{a,T}$ decreases), the sensitivity of Pr_t to ζ becomes more prominent, especially when $\zeta < 0$, as can be also seen from Fig. 5.

Interestingly, Fig. 4 also shows that, as the −1 power-law scaling in temperature spectra extends to lower K, the $\mathrm{Pr}_t^{-1}/\mathrm{Pr}_{t,\mathrm{neu}}^{-1}$–$\zeta$ relation becomes gradually different from the $\mathrm{Pr}_t^{-1}/\mathrm{Pr}_{t,\mathrm{neu}}^{-1}$–$R_g$ relation but resembles the $\mathrm{Pr}_t^{-1}/\mathrm{Pr}_{t,\mathrm{neu}}^{-1}$–$R_f$ relation. Furthermore, $\mathrm{Pr}_t^{-1}/\mathrm{Pr}_{t,\mathrm{neu}}^{-1}$ becomes near zero at a much lower ζ (<1) compared to the absence of a −1 scaling case. Similarly, Pr_t^{-1} approaches near zero at a lower R_f compared to the absence of a −1 scaling case. In summary, it appears that R_{fm} is reduced as the −1 power-law scaling regime extends to larger scales or lower K for air temperature spectra.

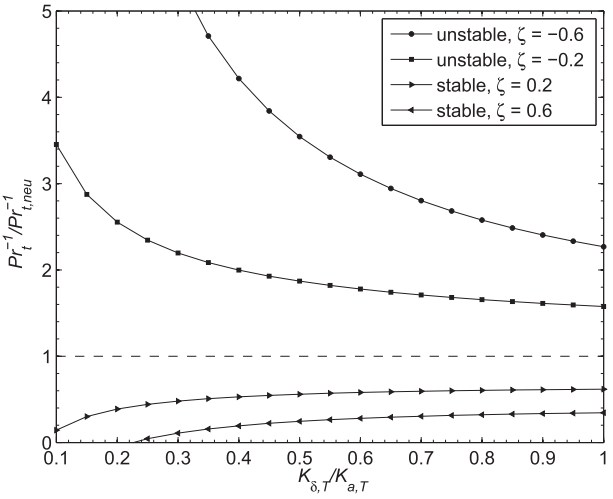

FIG. 5. $\mathrm{Pr}_t^{-1}/\mathrm{Pr}_{t,\mathrm{neu}}^{-1}$ as a function of $K_{\delta,T}/K_{a,T}$ under different stability conditions. Note that $\mathrm{Pr}_{t,\mathrm{neu}}$ is not affected by $K_{\delta,T}/K_{a,T}$.

c. *The impacts of flux transfer terms on* Pr_t

When compared to previous phenomenological models (Gioia et al. 2010; Katul et al. 2011; Salesky et al. 2013), the approach here allows investigation of the impacts of flux transfer terms on Pr_t. As mentioned earlier, the constants in the flux transfer terms affect $\mathrm{Pr}_{t,\mathrm{neu}}$. As such, before examining the impacts of flux transfer terms on Pr_t under thermally stratified conditions, their impacts on $\mathrm{Pr}_{t,\mathrm{neu}}$ are first presented. Under neutral conditions, Eqs. (32) and (33) can be simplified to

$$f_1 = \left[\frac{1}{(1+A_U/A_{UU})(1/3)} - \frac{1}{(1+A_U/A_{UU}-5/3)(1/3-5/3)}\right] K_{a,w}^{-4/3} \quad \text{and} \tag{42}$$

$$g_1 = \left[\frac{1}{(1+A_T/A_{TT})(1/3)} - \frac{1}{(1+A_T/A_{TT}-5/3)(1/3-5/3)}\right] K_{a,w}^{-4/3}. \tag{43}$$

As such,

$$\mathrm{Pr}_{t,\mathrm{neu}} = \frac{A_{TT}(1-C_{IU})}{A_{UU}(1-C_{IT})} \frac{\left[\dfrac{1}{(1+A_U/A_{UU})(1/3)} - \dfrac{1}{(1+A_U/A_{UU}-5/3)(1/3-5/3)}\right]}{\left[\dfrac{1}{(1+A_T/A_{TT})(1/3)} - \dfrac{1}{(1+A_T/A_{TT}-5/3)(1/3-5/3)}\right]}. \tag{44}$$

This expression can be further simplified into

$$\mathrm{Pr}_{t,\mathrm{neu}}^{-1} = \frac{A_U(1-C_{IT})}{A_T(1-C_{IU})} \times \frac{\left\{\dfrac{1}{(1+A_{TT}/A_T)} + \dfrac{1/4}{[1-(2/3)(A_{TT}/A_T)]}\right\}}{\left\{\dfrac{1}{(1+A_{UU}/A_U)} + \dfrac{1/4}{[1-(2/3)(A_{UU}/A_U)]}\right\}}. \tag{45}$$

It is clear that when $A_{UU} = 0$ and $A_{TT} = 0$, the above expression recovers the results of Katul et al. (2014). When $A_{UU} \neq 0$ and/or $A_{TT} \neq 0$, the neutral $\mathrm{Pr}_{t,\mathrm{neu}}^{-1}$ depends on the ratio of Rotta constants (A_U/A_T), the ratio of isotropization constants $[(1-C_{IT})/(1-C_{IU})]$, and the constants associated with the flux transfer terms normalized by the Rotta constants (A_{UU}/A_U and/or A_{TT}/A_T). Again, the departure of $\mathrm{Pr}_{t,\mathrm{neu}}$ from unity can result from $A_U \neq A_T$, $C_{IU} \neq C_{IT}$, or $A_{TT} \neq A_{UU}$. Interestingly, unlike A_U/A_T and $(1-C_{IT})/(1-C_{IU})$ that modulate $\mathrm{Pr}_{t,\mathrm{neu}}^{-1}$ linearly, the constants in the flux

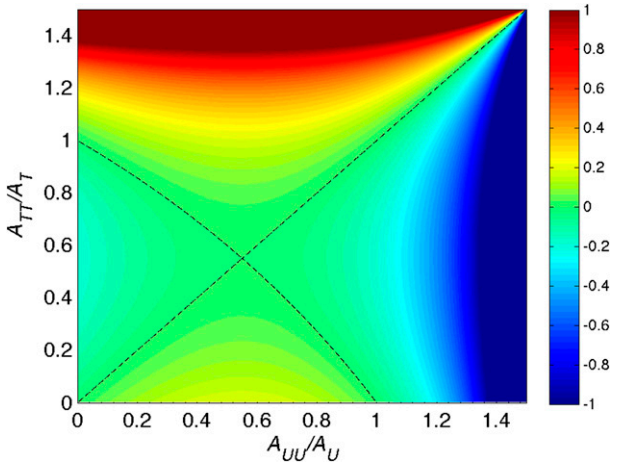

FIG. 6. Plot of $\ln(\mathrm{Pr}_{t,\mathrm{neu}}^{-1})$ as a function of A_{UU}/A_U and A_{TT}/A_T when $A_U/A_T = 1$ and $(1 - C_{IU})/(1 - C_{IT}) = 1$. The two black dashed lines denote the contour level $\ln(\mathrm{Pr}_{t,\mathrm{neu}}^{-1}) = 0$ or $\mathrm{Pr}_{t,\mathrm{neu}}^{-1} = 1$. The two black dashed lines intersect at $A_{UU}/A_U = A_{TT}/A_T \approx 0.55$. Note that $A_U/A_{UU} \geq \alpha - 1$ and $A_T/A_{TT} \geq \max(\alpha - 1, \gamma - 1)$, which leads to $0 \leq A_{UU}/A_U \leq 3/2$ and $0 \leq A_{TT}/A_T \leq 3/2$.

transfer terms modulate $\mathrm{Pr}_{t,\mathrm{neu}}^{-1}$ in a nonlinear manner. Figure 6 shows the $\ln(\mathrm{Pr}_{t,\mathrm{neu}}^{-1})$ as a function of A_{UU}/A_U and A_{TT}/A_T when $A_U/A_T = 1$ and $(1 - C_{IT})/(1 - C_{IU}) = 1$. There are two different situations that lead to $\ln(\mathrm{Pr}_{t,\mathrm{neu}}^{-1}) = 0$ or $\mathrm{Pr}_{t,\mathrm{neu}} = 1$: when $A_{UU} = A_{TT}$ or when $1/[(1 + A_{UU}/A_U)(1 + A_{TT}/A_T)] = (1/6)/\{[1 - (2/3)(A_{UU}/A_U)][1 - (2/3)(A_{TT}/A_T)]\}$, as shown by the two black dashed lines in Fig. 6 that intersect at $A_{TT}/A_T = A_{UU}/A_U = 3 - \sqrt{6} \approx 0.55$. For any value of A_{UU}/A_U, increasing A_{TT}/A_T will first reduce $\mathrm{Pr}_{t,\mathrm{neu}}^{-1}$ and then increase $\mathrm{Pr}_{t,\mathrm{neu}}^{-1}$ once A_{TT}/A_T exceeds 0.55. This suggests that a stronger flux transfer term in the heat flux budget will reduce the bulk heat transfer in ASL initially but increase the bulk heat transfer eventually. Similarly, a stronger flux transfer term in the momentum flux budget will reduce the bulk momentum transfer in ASL when $A_{UU}/A_U < 0.55$ and increase the bulk momentum transfer when $A_{UU}/A_U > 0.55$.

Figure 7 shows how dissimilarity in the flux transfer terms alter the $\mathrm{Pr}_t^{-1}/\mathrm{Pr}_{t,\mathrm{neu}}^{-1}$–$\zeta$, $\mathrm{Pr}_t^{-1}/\mathrm{Pr}_{t,\mathrm{neu}}^{-1}$–$R_g$, and $\mathrm{Pr}_t^{-1}/\mathrm{Pr}_{t,\mathrm{neu}}^{-1}$–$R_f$ relations when these flux transfer terms are significant (i.e., when A_{UU}/A_U and A_{TT}/A_T are larger than 0.55; see Figs. 7a–c) and when they are not important (i.e., A_{UU}/A_U and A_{TT}/A_T are smaller than 0.55; see Figs. 7d–f). It is clear that the dependence of Pr_t^{-1} on stability is not significantly altered by the dissimilarity in the flux transfer terms, even when these flux transfer terms are significant. This indicates that dissimilarity in the flux transfer terms affects Pr_t^{-1} by affecting $\mathrm{Pr}_{t,\mathrm{neu}}^{-1}$, but not through Q. Nevertheless, it is noted here that, although the sensitivities of $\mathrm{Pr}_t^{-1}/\mathrm{Pr}_{t,\mathrm{neu}}^{-1}$ to A_{UU}/A_{TT} are small, the relations $\mathrm{Pr}_t^{-1}/\mathrm{Pr}_{t,\mathrm{neu}}^{-1}$–$\zeta$ and $\mathrm{Pr}_t^{-1}/\mathrm{Pr}_{t,\mathrm{neu}}^{-1}$–$R_f$ seems to be sensitive to A_{UU}/A_{TT} under free-convective conditions, while the relation $\mathrm{Pr}_t^{-1}/\mathrm{Pr}_{t,\mathrm{neu}}^{-1}$–$R_g$ is sensitive to A_{UU}/A_{TT} under slightly unstable conditions.

The significance of the flux transfer terms does not necessarily imply that the flux transport terms in the flux budget equations [Eqs. (7) and (8)] are significant. In fact, the gradient diffusion closure employed in the spectral domain for $T_{uw}(K)$ and $T_{wT}(K)$ ensures $\int_0^\infty T_{uw}(K)\,dK = 0$ and $\int_0^\infty T_{wT}(K)\,dK = 0$. That is, $T_{uw}(K)$ and $T_{wT}(K)$ simply redistribute covariances across K but do not produce or dissipate them thereby preserving the constant flux approximation in an idealized ASL flow.

d. The maximum flux Richardson number

As noted earlier, the maximum flux Richardson number is interpreted as a threshold above which stationarity, advection, subsidence, and flux transport terms cannot remain insignificant with further increases in R_f in the ASL. Moreover, the idealized shapes (especially Kolmogorov scaling and other scaling laws at low wavenumbers) of the vertical velocity and temperature spectra assumed here break down with further increases in R_f beyond R_{fm}. A recent long-term experiment already showed that when $R_f > 0.2$–0.25, Kolmogorov scaling no longer holds in temperature and vertical velocity spectra (Grachev et al. 2013). So, the focus of this section is restricted to how the flux transfer terms and possible existence of a -1 power-law scaling in temperature spectra shift the magnitude of an R_{fm}. We do not explore the turbulent state for $R_f > R_{fm}$, because the idealized state of the ASL and concomitant constant flux assumptions become questionable, and the idealized spectral shapes for temperature and vertical velocity previously assumed in Fig. 1 no longer hold.

The magnitude of R_{fm} is affected by the occurrence of a -1 power-law scaling in the air temperature spectra and by the flux transfer terms. Interestingly, the flux transfer terms affect the maximum flux Richardson number only through A_{TT}, not A_{UU}. This is because R_{fm} is affected by g_2/g_1 when C_{IT} and C_T/C_o are specified [see Eq. (41)], but A_{UU} is affecting neither g_1 nor g_2. In addition, only when $K_{\delta,T} \neq K_{a,T}$ is $g_2 \neq g_1$ and is R_{fm} dependent on A_{TT}/A_T, as shown in Fig. 8. When a -1 power-law scaling regime in the air temperature spectrum exists, the flux transfer term in the cospectral budget of heat flux affects R_{fm}. Again, as the -1 power-law scaling extends to lower K, R_{fm} is reduced consistent with Fig. 4. When compared with the possible existence of a -1 power-law scaling regime reducing R_{fm}, increasing A_{TT} compensates for the reduced R_{fm} and turns

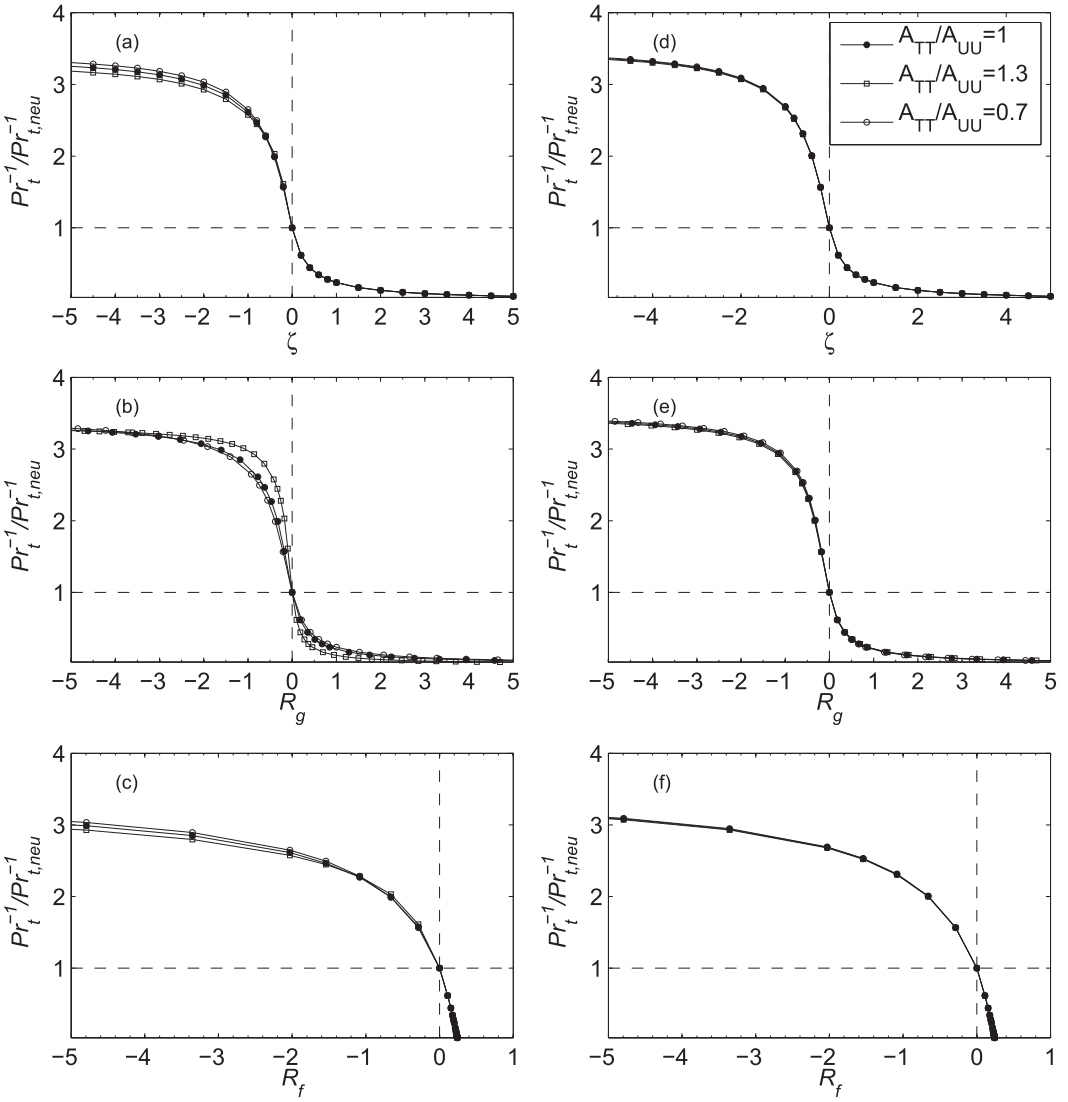

FIG. 7. $\mathrm{Pr}_t^{-1}/\mathrm{Pr}_{t,\mathrm{neu}}^{-1}$ as a function of (a),(d) $\zeta = z/L$; (b),(e) R_g; and (c),(f) R_f when dissimilarity exists between the flux transfer terms in momentum and heat flux cospectral budgets. $K_{\delta,T} = K_{a,T}$ is assumed here, but other values of $K_{\delta,T} = K_{a,T}$ also yield similar results, except that the maximum flux Richardson number is altered by the inequality between $K_{\delta,T}$ and $K_{a,T}$, as in Fig. 8. In (a)–(c), $A_{UU}/A_U = 1 > 0.55$ is used, while in (d)–(f), $A_{UU}/A_U = 0.3 < 0.55$ is used.

it back to its value when $K_{\delta,T} = K_{a,T}$. Hence, it can be conjectured that the flux transfer term in the heat flux budget mediates the impact of the -1 power-law scaling in air temperature spectra on R_{fm}.

4. Conclusions and discussion

A recently proposed cospectral budget method that links kinetic energy of eddies in the vertical direction via $F_{ww}(K)$ and their potential energy via $F_{TT}(K)$ to macroscopic relations, such as Pr_t–ζ (or Pr_t–R_g), is generalized here to accommodate extensions of the $-5/3$ power-law scaling in both vertical velocity and air temperature spectra for free-convective conditions, the possible existence of -1 power-law scaling in air temperature spectra under near-neutral and mildly stable conditions, and the existence of finite flux transfer terms. The generalized model reproduces the Pr_t–ζ relation under unstable conditions and the Pr_t–R_g relation under stable conditions reported in many experiments and simulations. Pr_t^{-1} is shown to decrease with ζ or R_g, implying that heat is transferred less efficiently than momentum as stability increases. This does not contradict several experimental studies showing that Pr_t^{-1}

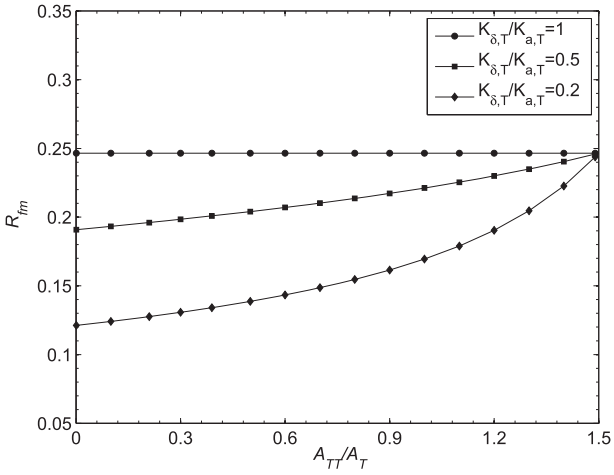

FIG. 8. The variation of R_{fm} with increasing contributions from the flux transfer terms represented by A_{TT}/A_T under different $K_{\delta,T}/K_{a,T}$ conditions.

decreases with R_g but increases with ζ under stable conditions because of self-correlation.

It is shown that the dependence of Pr_t on stability is primarily controlled by the ratio of the Kolmogorov and the Kolmogorov–Obukhov–Corrsin phenomenological constants (C_o/C_T) and a constant associated with the isotropization of the production C_{IT}, the value of which can be determined from rapid distortion theory in homogeneous turbulence (=3/5). Changes in scaling laws of the vertical velocity and air temperature spectra that represent the kinetic and potential energy distributions of turbulent eddies, respectively, also affect the Pr_t–ζ or Pr_t–R_g relation. For example, the extension of the $-5/3$ power-law scaling in the vertical velocity spectrum reduces the Pr_t under free-convective conditions. The possible existence of -1 power-law scaling in the air temperature spectrum significantly increases the sensitivity of Pr_t to ζ for near-neutral conditions.

However, unlike changes in these scaling laws in the vertical velocity and air temperature spectra affecting the stability impact on Pr_t, dissimilarity in the flux transfer terms in momentum and heat flux cospectral budgets primarily alter Pr_t for near-neutral conditions $\mathrm{Pr}_{t,\mathrm{neu}}$ but not the $\mathrm{Pr}_t/\mathrm{Pr}_{t,\mathrm{neu}}$–$\zeta$ or $\mathrm{Pr}_t/\mathrm{Pr}_{t,\mathrm{neu}}$–$R_g$ relation. It is to be noted that the impacts of flux transfer terms on anomalous scaling within the inertial subrange of momentum and heat flux cospectra are excluded by setting $E_1 = 0$ and $E_2 = 0$ in Eqs. (24) and (25), respectively, thereby ensuring that such cospectra maintain a $K^{-7/3}$ scaling exponent. Nonetheless, this restriction, while in agreement with numerous cospectral measurements in the ASL, implies that the impacts of flux transfer terms are not fully accounted for.

The Pr_t–R_f relation is shown to significantly differ from the Pr_t–ζ relation or the Pr_t–R_g relation because of the presence of a maximum flux Richardson number R_{fm}. The cospectral budgets method correctly predicted its onset and yielded a value of R_{fm} ($\approx$0.25), consistent with those reported in the literature. Model results further suggest that both the possible -1 power-law scaling in the air temperature spectra and the flux transfer term in the heat flux cospectral budget affect the value of R_{fm}. Possible existence of the -1 power-law scaling reduces the value of R_{fm}, while the flux transfer term in the heat flux cospectral budget counters this reduction.

More broadly, such linkages between the energy distributions of turbulent eddies (both kinetic and potential) encoded in the spectra and macroscopic relations of the mean flow such as Pr_t–R_f, Pr_t–ζ, or Pr_t–R_g may offer new perspectives as to when dimensional considerations and similarity theory are expected to hold. This perspective may explain why similarity theories work well for unstable and moderately stable ASL flows but not for very stable ASL flows, presumably as a result of the collapse of the spectral shapes from their idealized assumptions with increasing stability.

In addition, under stable conditions, the cospectral budget model and the energy- and flux-budget (EFB) turbulence closure model proposed by Zilitinkevich et al. (2007, 2008, 2013) both capture the Pr_t–R_g relation reasonably well. The EFB turbulence closure model specifies the ratio of turbulent kinetic energy and turbulent potential energy with stability, while the cospectral budget model predicts this ratio using prespecified shapes of vertical velocity and air temperature spectra. Agreement between these two seemingly separate approaches suggests novel ways to connect the underlying physics for ordinary closure schemes and spectral shapes, thereby providing new constraints on empirical closure constants. Future investigations are needed to examine other connections between these two approaches.

Acknowledgments. D. L. acknowledges support from the NOAA (U.S. Department of Commerce) Grant NA08OAR4320752 and the Carbon Mitigation Initiative at Princeton University, sponsored by BP. The statements, findings, and conclusions are those of the authors and do not necessarily reflect the views of the NOAA, the U.S. Department of Commerce, or BP. G. K. acknowledges support from the U.S. National Science Foundation (NSF-EAR-1344703 and NSF-AGS-1102227), the U.S. Department of Energy (DOE) through the Office of Biological and Environmental Research (BER) Terrestrial Carbon Processes (TCP) program (DE-SC0006967 and DE-SC0011461), and the Agriculture and Food Research Initiative from the USDA National Institute of Food and Agriculture (2011-67003-30222). S. Z. acknowledges support from

the European Commission ERC-Ideas PoC Project 632295-INMOST (2014–15); the Academy of Finland project ABBA, Contract 280700 (2014–17); the Russian Mega-grant Contract 11.G34.31.0048 (2011–15); and the Russian Federal Program—Research and Development on priority directions of development of scientific–technological infrastructure of Russia for 2014–20, Contract 14.578.21.0033 (2014–16).

REFERENCES

Anderson, P. S., 2009: Measurement of Prandtl number as a function of Richardson number avoiding self-correlation. *Bound.-Layer Meteor.,* **131,** 345–362, doi:10.1007/s10546-009-9376-4.

Andren, A., 1995: The structure of stably stratified atmospheric boundary layers: A large eddy simulation study. *Quart. J. Roy. Meteor. Soc.,* **121,** 961–985, doi:10.1002/qj.49712152502.

Baldocchi, D., and Coauthors, 2001: FLUXNET: A new tool to study the temporal and spatial variability of ecosystem-scale carbon dioxide, water vapor, and energy flux densities. *Bull. Amer. Meteor. Soc.,* **82,** 2415–2434, doi:10.1175/1520-0477(2001)082<2415:FANTTS>2.3.CO;2.

Banerjee, T., and G. Katul, 2013: Logarithmic scaling in the longitudinal velocity variance explained by a spectral budget. *Phys. Fluids,* **25,** 125106, doi:10.1063/1.4837876.

Bodenschatz, E., S. P. Malinowski, R. A. Shaw, and F. Stratmann, 2010: Can we understand clouds without turbulence? *Science,* **327,** 970–971, doi:10.1126/science.1185138.

Bos, W., and J. Bertoglio, 2007: Inertial range scaling of scalar flux spectra in uniformly sheared turbulence. *Phys. Fluids,* **19,** 025104, doi:10.1063/1.2565563.

——, H. Touil, L. Shao, and J. Bertogli, 2004: On the behavior of the velocity-scalar cross correlation spectrum in the inertial range. *Phys. Fluids,* **16,** 3818–3823, doi:10.1063/1.1779229.

Bou-Zeid, E., N. Vercauteren, M. Parlange, and C. Meneveau, 2008: Scale dependence of subgrid-scale model coefficients: An a priori study. *Phys. Fluids,* **20,** 115106, doi:10.1063/1.2992192.

Brutsaert, W. B., 1982: *Evaporation into the Atmosphere.* Kluwer Academic Publishers, 299 pp.

——, 2005: *Hydrology: An Introduction*. Cambridge University Press, 605 pp.

Businger, J. A., 1988: A note on the Businger–Dyer profiles. *Bound.-Layer Meteor.,* **42,** 145–151, doi:10.1007/BF00119880.

——, and A. M. Yaglom, 1971: Introduction to Obukhov's paper on 'Turbulence in an atmosphere with a non-uniform temperature.' *Bound.-Layer Meteor.,* **2,** 3–6, doi:10.1007/BF00718084.

——, J. C. Wyngaard, Y. Izumi, and E. F. Bradley, 1971: Flux-profile relationships in the atmospheric surface layer. *J. Atmos. Sci.,* **28,** 181–191, doi:10.1175/1520-0469(1971)028<0181:FPRITA>2.0.CO;2.

Canuto, V. M., Y. Cheng, A. Howard, and I. Esau, 2008: Stably stratified flows: A model with no Ri(cr). *J. Atmos. Sci.,* **65,** 2437–2447, doi:10.1175/2007JAS2470.1.

Cava, D., and G. Katul, 2012: On the scaling laws of the velocity-scalar cospectra in the canopy sublayer above tall forests. *Bound.-Layer Meteor.,* **145,** 351–367, doi:10.1007/s10546-012-9737-2.

Charuchittipan, D., and J. Wilson, 2009: Turbulent kinetic energy dissipation in the surface layer. *Bound.-Layer Meteor.,* **132,** 193–204, doi:10.1007/s10546-009-9399-x.

Choi, K., and J. Lumley, 2001: The return to isotropy of homogeneous turbulence. *J. Fluid Mech.,* **436,** 59–84, doi:10.1017/S002211200100386X.

Chung, D., and G. Matheou, 2012: Direct numerical simulation of stationary homogeneous stratified sheared turbulence. *J. Fluid Mech.,* **696,** 434–467, doi:10.1017/jfm.2012.59.

Corrsin, S., 1961: The reactant concentration spectrum in turbulent mixing with a first-order reaction. *J. Fluid Mech.,* **11,** 407–416, doi:10.1017/S0022112061000615.

Esau, I., and A. A. Grachev, 2007: Turbulent Prandtl number in stably stratified atmospheric boundary layer: Intercomparison between LES and SHEBA data. *e-WindEng,* **006,** 1–17. [Available online at http://ejournal.windeng.net/16/.]

Galperin, B., S. Sukoriansky, and P. S. Anderson, 2007: On the critical Richardson number in stably stratified turbulence. *Atmos. Sci. Lett.,* **8,** 65–69, doi:10.1002/asl.153.

Gioia, G., N. Guttenberg, N. Goldenfeld, and P. Chakraborty, 2010: Spectral theory of the turbulent mean-velocity profile. *Phys. Rev. Lett.,* **105,** 184501, doi:10.1103/PhysRevLett.105.184501.

Grachev, A., E. Andreas, C. Fairall, P. Guest, and P. G. Persson, 2007: On the turbulent Prandtl number in the stable atmospheric boundary layer. *Bound.-Layer Meteor.,* **125,** 329–341, doi:10.1007/s10546-007-9192-7.

——, ——, ——, ——, and ——, 2013: The critical Richardson number and limits of applicability of local similarity theory in the stable boundary layer. *Bound.-Layer Meteor.,* **147,** 51–82, doi:10.1007/s10546-012-9771-0.

Guala, M., M. Metzger, and B. McKeon, 2010: Intermittency in the atmospheric surface layer: Unresolved or slowly varying? *Physica D,* **239,** 1251–1257, doi:10.1016/j.physd.2009.10.010.

Högström, U., 1988: Non-dimensional wind and temperature profiles in the atmospheric surface layer: A re-evaluation. *Bound.-Layer Meteor.,* **42,** 55–78, doi:10.1007/BF00119875.

Howard, L. N., 1961: Note on a paper of John W. Miles. *J. Fluid Mech.,* **10,** 509–512, doi:10.1017/S0022112061000317.

Hsieh, C.-I., and G. G. Katul, 1997: Dissipation methods, Taylor's hypothesis, and stability correction functions in the atmospheric surface layer. *J. Geophys. Res.,* **102,** 16 391–16 405, doi:10.1029/97JD00200.

Hutchins, N., K. Chauhan, I. Marusic, J. Monty, and J. Klewicki, 2012: Towards reconciling the large-scale structure of turbulent boundary layers in the atmosphere and laboratory. *Bound.-Layer Meteor.,* **145,** 273–306, doi:10.1007/s10546-012-9735-4.

Ishihara, T., K. Yoshida, and Y. Kaneda, 2002: Anisotropic velocity correlation spectrum at small scales in a homogeneous turbulent shear flow. *Phys. Rev. Lett.,* **88,** 154501, doi:10.1103/PhysRevLett.88.154501.

Kader, B. A., and A. M. Yaglom, 1990: Mean fields and fluctuation moments in unstably stratified turbulent boundary layers. *J. Fluid Mech.,* **212,** 637–662, doi:10.1017/S0022112090002129.

——, and ——, 1991: Spectra and correlation functions of surface layer atmospheric turbulence in unstable thermal stratification. *Turbulence and Coherent Structures,* O. Metais and M. Lesieur, Eds., Fluid Mechanics and Its Applications, Vol. 2, Kluwer Academic Publishers, 387–412, doi:10.1007/978-94-015-7904-9_24.

Kaimal, J. C., 1973: Turbulence spectra, length scales and structure parameters in the stable surface layer. *Bound.-Layer Meteor.,* **4,** 289–309, doi:10.1007/BF02265239.

——, and J. Finnigan, 1994: *Atmospheric Boundary Layer Flows: Their Structure and Measurement.* Oxford University Press, 289 pp.

——, Y. Izumi, J. C. Wyngaard, and R. Cote, 1972: Spectral characteristics of surface-layer turbulence. *Quart. J. Roy. Meteor. Soc.,* **98,** 563–589, doi:10.1002/qj.49709841707.

Katul, G. G., and C. Chu, 1998: A theoretical and experimental investigation of energy-containing scales in the dynamic sublayer of boundary-layer flows. *Bound.-Layer Meteor.,* **86,** 279–312, doi:10.1023/A:1000657014845.

——, and C. Manes, 2014: Cospectral budget of turbulence explains the bulk properties of smooth pipe flow. *Phys. Rev.,* **90E,** 063008, doi:10.1103/PhysRevE.90.063008.

——, C. Chu, M. Parlange, J. Albertson, and T. Ortenburger, 1995: Low-wavenumber spectral characteristics of velocity and temperature in the atmospheric surface layer. *J. Geophys. Res.,* **100,** 14 243–14 255, doi:10.1029/94JD02616.

——, J. Albertson, C. Hsieh, P. Conklin, J. Sigmon, M. Parlange, and K. Knoerr, 1996: The ''inactive'' eddy motion and the large-scale turbulent pressure fluctuations in the dynamic sublayer. *J. Atmos. Sci.,* **53,** 2512–2524, doi:10.1175/1520-0469(1996)053<2512:TEMATL>2.0.CO;2.

——, A. Konings, and A. Porporato, 2011: Mean velocity profile in a sheared and thermally stratified atmospheric boundary layer. *Phys. Rev. Lett.,* **107,** 268502, doi:10.1103/PhysRevLett.107.268502.

——, A. Porporato, and V. Nikora, 2012: Existence of k^{-1} power-law scaling in the equilibrium regions of wall-bounded turbulence explained by Heisenberg's eddy viscosity. *Phys. Rev.,* **86E,** 066311, doi:10.1103/PhysRevE.86.066311.

——, D. Li, M. Chamecki, and E. Bou-Zeid, 2013a: Mean scalar concentration profile in a sheared and thermally stratified atmospheric surface layer. *Phys. Rev.,* **87E,** 023004, doi:10.1103/PhysRevE.87.023004.

——, A. Porporato, C. Manes, and C. Meneveau, 2013b: Co-spectrum and mean velocity in turbulent boundary layers. *Phys. Fluids,* **25,** 091702, doi:10.1063/1.4821997.

——, ——, S. Shah, and E. Bou-Zeid, 2014: Two phenomenological constants explain similarity laws in stably stratified turbulence. *Phys. Rev.,* **89E,** 023007, doi:10.1103/PhysRevE.89.023007.

Kays, W., 1994: Turbulent Prandtl number—Where are we? *J. Heat Transfer,* **116,** 284–295, doi:10.1115/1.2911398.

Klipp, C. L., and L. Mahrt, 2004: Flux-gradient relationship, self-correlation and intermittency in the stable boundary layer. *Quart. J. Roy. Meteor. Soc.,* **130,** 2087–2103, doi:10.1256/qj.03.161.

Kolmogorov, A., 1941: Dissipation of energy under locally isotropic turbulence. *Dokl. Akad. Nauk SSSR,* **32,** 16–18.

Launder, B., G. Reece, and W. Rodi, 1975: Progress in the development of a Reynolds-stress turbulence closure. *J. Fluid Mech.,* **68,** 537–566, doi:10.1017/S0022112075001814.

Li, D., and E. Bou-Zeid, 2011: Coherent structures and the dissimilarity of turbulent transport of momentum and scalars in the unstable atmospheric surface layer. *Bound.-Layer Meteor.,* **140,** 243–262, doi:10.1007/s10546-011-9613-5.

——, G. G. Katul, and E. Bou-Zeid, 2012: Mean velocity and temperature profiles in a sheared diabatic turbulent boundary layer. *Phys. Fluids,* **24,** 105105, doi:10.1063/1.4757660.

Lilly, D., 1992: A proposed modification of the Germano subgrid-scale closure method. *Phys. Fluids,* **4,** 633, doi:10.1063/1.858280.

Marusic, I., B. J. McKeon, P. A. Monkewitz, H. M. Nagib, A. J. Smits, and K. R. Sreenivasan, 2010: Wall-bounded turbulent flows at high Reynolds numbers: Recent advances and key issues. *Phys. Fluids,* **22,** 065103, doi:10.1063/1.3453711.

McNaughton, K. G., and J. Laubach, 2000: Power spectra and co-spectra for wind and scalars in a disturbed surface layer at the base of an advective inversion. *Bound.-Layer Meteor.,* **96,** 143–185, doi:10.1023/A:1002477120507.

——, and Y. Brunet, 2002: Townsend's hypothesis, coherent structures and Monin–Obukhov similarity. *Bound.-Layer Meteor.,* **102,** 161–175, doi:10.1023/A:1013171312407.

Mellor, G., and T. Yamada, 1974: A hierarchy of turbulence closure models for planetary boundary layers. *J. Atmos. Sci.,* **31,** 1791–1806, doi:10.1175/1520-0469(1974)031<1791:AHOTCM>2.0.CO;2.

Miles, J. W., 1961: On the stability of heterogeneous shear flows. *J. Fluid Mech.,* **10,** 496–508, doi:10.1017/S0022112061000305.

Monin, A., and A. Obukhov, 1954: Basic laws of turbulent mixing in the ground layer of the atmosphere. *Tr. Geofiz. Inst. Akad. Nauk. SSSR,* **151,** 163–187.

——, and A. Yaglom, 1971: *Statistical Fluid Mechanics: Mechanics of Turbulence; Volume 1*. MIT Press, 873 pp.

Moraes, O., 2000: Turbulence characteristics in the surface boundary layer over the South American Pampa. *Bound.-Layer Meteor.,* **96,** 317–335, doi:10.1023/A:1002604624749.

Obukhov, A., 1946: Turbulence in thermally inhomogeneous atmosphere. *Tr. Inst. Teor. Geofiz. Akad. Nauk SSSR,* **1,** 95–115.

Ohya, Y., 2001: Wind-tunnel study of atmospheric stable boundary layers over a rough surface. *Bound.-Layer Meteor.,* **98,** 57–82, doi:10.1023/A:1018767829067.

Panchev, S., 1971: *Random Functions and Turbulence. Int. Ser. Monogr. Nat. Philos.,* Vol. 32, Pergamon Press, 444 pp.

Pond, S., S. Smith, P. Hamblin, and R. Burling, 1966: Spectra of velocity and temperature fluctuations in the atmospheric boundary layer over the sea. *J. Atmos. Sci.,* **23,** 376–386, doi:10.1175/1520-0469(1966)023<0376:SOVATF>2.0.CO;2.

Pope, S., 2000: *Turbulent Flows.* Cambridge University Press, 771 pp.

Reynolds, A., 1975: The prediction of turbulent Prandtl and Schmidt numbers. *Int. J. Heat Mass Transfer,* **18,** 1055–1069, doi:10.1016/0017-9310(75)90223-9.

Rodrigo, J. S., and P. S. Anderson, 2013: Investigation of the stable atmospheric boundary layer at Halley Antarctica. *Bound.-Layer Meteor.,* **148,** 517–539, doi:10.1007/s10546-013-9831-0.

Rohr, J. J., E. C. Itsweire, K. N. Helland, and C. W. Van Atta, 1988: Growth and decay of turbulence in a stably stratified shear flow. *J. Fluid Mech.,* **195,** 77–111, doi:10.1017/S0022112088002332.

Salesky, S. T., G. G. Katul, and M. Chamecki, 2013: Buoyancy effects on the integral lengthscales and mean velocity profile in atmospheric surface layer flows. *Phys. Fluids,* **25,** 105101, doi:10.1063/1.4823747.

Shah, S. K., and E. Bou-Zeid, 2014: Direct numerical simulations of turbulent Ekman layers with increasing static stability: Modifications to the bulk structure and second-order statistics. *J. Fluid Mech.,* **760,** 494–539, doi:10.1017/jfm.2014.597.

Shih, L., J. Koseff, J. Ferziger, and C. Rehmann, 2000: Scaling and parameterization of stratified homogeneous turbulent shear flow. *J. Fluid Mech.,* **412,** 1–20, doi:10.1017/S0022112000008405.

Smedman, A., U. Högström, J. Hunt, and E. Sahlee, 2007: Heat/mass transfer in the slightly unstable atmospheric surface layer. *Quart. J. Roy. Meteor. Soc.,* **133,** 37–51, doi:10.1002/qj.7.

Smits, A. J., B. J. McKeon, and I. Marusic, 2011: High-Reynolds number wall turbulence. *Annu. Rev. Fluid Mech.,* **43,** 353–375, doi:10.1146/annurev-fluid-122109-160753.

Sreenivasan, K. R., 1995: On the universality of the Kolmogorov constant. *Phys. Fluids,* **7,** 2778–2784, doi:10.1063/1.868656.

——, 1996: The passive scalar spectrum and the Obukhov–Corrsin constant. *Phys. Fluids,* **8,** 189–196, doi:10.1063/1.868826.

Stensrud, D., 2007: *Parameterization Schemes: Keys to Understanding Numerical Weather Prediction Models.* Cambridge University Press, 459 pp.

Stretch, D., J. Rottman, S. Venayagamoorthy, K. K. Nomura, and C. R. Rehmann, 2010: Mixing efficiency in decaying stably stratified turbulence. *Dyn. Atmos. Oceans,* **49,** 25–36, doi:10.1016/j.dynatmoce.2008.11.002.

Stull, R., 1988: *An Introduction to Boundary Layer Meteorology.* Kluwer Academic Publishers, 670 pp.

Taylor, G., 1938: The spectrum of turbulence. *Proc. Roy. Soc. London,* **A132,** 476–490, doi:10.1098/rspa.1938.0032.

Webster, C., 1964: An experimental study of turbulence in a density-stratified shear flow. *J. Fluid Mech.,* **19,** 221–245, doi:10.1017/S0022112064000672.

Wyngaard, J., and O. Cote, 1972: Cospectral similarity in the atmospheric surface layer. *Quart. J. Roy. Meteor. Soc.,* **98,** 590–603, doi:10.1002/qj.49709841708.

Yakhot, V., S. A. Orszag, and A. Yakhot, 1987: Heat transfer in turbulent fluids—I. Pipe flow. *Int. J. Heat Mass Transfer,* **30,** 15–22, doi:10.1016/0017-9310(87)90057-3.

Yamada, T., 1975: The critical Richardson number and the ratio of the eddy transport coefficients obtained from a turbulence closure model. *J. Atmos. Sci.,* **32,** 926–933, doi:10.1175/1520-0469(1975)032<0926:TCRNAT>2.0.CO;2.

Yeung, P., and Y. Zhou, 1997: Universality of the Kolmogorov constant in numerical simulations of turbulence. *Phys. Rev.,* **56E,** 1746, doi:10.1103/PhysRevE.56.1746.

Zilitinkevich, S., T. Elperin, N. Kleeorin, and I. Rogachevskii, 2007: Energy- and flux-budget (EFB) turbulence closure model for stably stratified flows. Part I: Steady-state, homogeneous regimes. *Bound.-Layer Meteor.,* **125,** 167–192, doi:10.1007/s10546-007-9189-2.

——, ——, ——, ——, I. Esau, T. Mauritsen, and M. Miles, 2008: Turbulence energetics in stably stratified geophysical flows: Strong and weak mixing regimes. *Quart. J. Roy. Meteor. Soc.,* **134,** 793–799, doi:10.1002/qj.264.

——, ——, ——, ——, and ——, 2013: A hierarchy of energy- and flux-budget (EFB) turbulence closure models for stably-stratified geophysical flows. *Bound.-Layer Meteor.,* **146,** 341–373, doi:10.1007/s10546-012-9768-8.

Zúñiga Zamalloa, C., H. C.-H. Ng, P. Chakraborty, and G. Gioia, 2014: Spectral analogues of the law of the wall, the defect law and the log law. *J. Fluid Mech.,* **757,** 498–513, doi:10.1017/jfm.2014.497.